Arabian Journal of Chemistry (2022) **15**, 104336

King Saud University

Arabian Journal of Chemistry

www.ksu.edu.sa
www.sciencedirect.com

ORIGINAL ARTICLE

A robust computational investigation on C60 fullerene nanostructure as a novel sensor to detect SCN^-

Saad M. Alshahrani [a], Sameer Alshehri [b], Amal M. Alsubaiyel [c], Rami M. Alzhrani [b], Ahmed D. Alatawi [d], Majed Ahmed Algarni [e], Maram H. Abduljabbar [f], Andrew Ng Kay Lup [g,h,*], Mohd Sani Sarjad [i], Md. Lutfor Rahman [i,*], Mohammed A.S. Abourehab [j,k]

[a] *Department of Pharmaceutics, College of Pharmacy, Prince Sattam Bin Abdulaziz University, P.O. Box 173, Al-Kharj 11942, Saudi Arabia*
[b] *Department of Pharmaceutics and Industrial Pharmacy, College of Pharmacy, Taif University, P.O. Box 11099, Taif 21944, Saudi Arabia*
[c] *Department of Pharmaceutics, College of Pharmacy, Qassim University, Buraidah 52571, Saudi Arabia*
[d] *Department of Clinical Pharmacy, College of Pharmacy, Jouf University, Sakaka, Al-Jouf, Saudi Arabia*
[e] *Department of Clinical Pharmacy, College of Pharmacy, Taif University, P.O. Box 11099, Taif 21944, Saudi Arabia*
[f] *Department of Pharmacology and Toxicology, College of Pharmacy, Taif University, Taif 21944, Saudi Arabia*
[g] *School of Energy and Chemical Engineering, Xiamen University Malaysia, Jalan Sunsuria, Bandar Sunsuria, 43900 Sepang, Selangor Darul Ehsan, Malaysia*
[h] *College of Chemistry and Chemical Engineering, Xiamen University, Xiamen 361005, Fujian, China*
[i] *Faculty of Science and Natural Resources, Universiti Malaysia Sabah, Kota Kinabalu 88400, Sabah, Malaysia*
[j] *Department of Pharmaceutics, College of Pharmacy, Umm Al-Qura University, Makkah 21955, Saudi Arabia*
[k] *Department of Pharmaceutics and Industrial Pharmacy, Faculty of Pharmacy, Minia University, Minia 61519, Egypt*

Received 20 June 2022; accepted 5 October 2022
Available online 10 October 2022

KEYWORDS

C_{60} fullerene;
Adsorption;
Density functional theory;

Abstract This study explored on the adsorption properties and electronic structure of SCN^- via density functional theory analysis on the exterior surfaces of C_{60} and CNTs using B3LYP functional and 6-31G** standard basis set. Then adsorption of SCN^- through nitrogen atom on the C_{60} fullerene is electrostatic (−48.02 kJ mol^{-1}) in comparison with the $C_{59}Al$ fullerene that shows

* Corresponding authors.
E-mail addresses: andrew.ng@xmu.edu.my (A. Ng Kay Lup), lotfor@ums.edu.my (M.L. Rahman).
Peer review under responsibility of King Saud University.

Production and hosting by Elsevier

https://doi.org/10.1016/j.arabjc.2022.104336

SCN

covalently attached to fullerene surface (−389.10 kJ mol^{-1}). Our calculations demonstrate that the SCN^- adsorption on the pristine and Al-doped single-walled CNTs are −173.13 and −334.43 kJ mol^{-1}, indicating that the SCN^- can be chemically bonded on the surface of Al-doped CNTs. Moreover, the adsorption of SCN^- on the C_{60} surface is weaker in comparison with $C_{59}B$, $C_{59}Al$, and $C_{59}Ga$ systems but its electronic sensitivity improved in comparison with those of $C_{59}B$, $C_{59}Al$, and $C_{59}Ga$ fullerenes. The evaluation of adsorption energy, energy gap, and dipole moment demonstrates that the pure fullerene can be exploited in the design practice as an SCN^- sensor and $C_{59}Al$ can be used for SCN^- removal applications.

1. Introduction

Over these past decades, various carbon based structures have been found such as C_{60} fullerene by Kroto et al. (1985) in 1985 and SWCNTs through Iijima (1991) in 1991, encouraging scientists to have drastic attention on their chemical, physical, mechanical, and electronical phenomena of these novel materials. Due to technological availability, the most ample C_{60} molecule has the most widely adaptation of fullerenes. Thus, it has been of the most focused material to be under research by various chemists of their research areas, including gas storage, pharmaceutical studies, batteries, transistors, sensors and micro-electromechanical systems and sensor applications, due to its exclusive properties of unusual stability, superconductivity, ferroelectricity, non-linear optical properties, ultra-stiffness to ferromagnetism (Ren et al., 2006; Krainara et al., 2012; Sabirov et al., 2008; Liu, 2009; Rondeau-Gagne et al., 2010; Funasaka et al., 1995; Wilson, 1999; Bakry et al., 2007).

Fullerene, particularly C_{60}, has been used as a good electron acceptor without changes to its electronic properties during its chemical bonding with other organic molecules (Liu et al., 2008; Shinohara, 2000). Hetero fullerenes have been the source of attention both experimentally and theoretically (Shi et al., 2016; Bezi Javan et al., 2010; Neyts et al., 2011). Doping inside of the fullerene molecule and substitute of heteroatoms (hetero fullerene) with one or more carbon atoms of the molecules of fullerene are two approaches of doping on C_{60}. Abundant experimental investigations for endohedrally doped or exohedrally doped fullerenes via metal atoms were performed. Among them, the point of interest has been given to cage structures endohedrally doped with many atoms including some gases, transition metallic, and rare earth atoms (Ren et al., 2008; Murata et al., 2006; Mauser et al., 1997; Larssona and Greer, 2002). The interaction properties between gas molecules and fullerene-doped structures are known among scientists as one of the most important aspects when considering intermolecular interactions (Hernández et al., 2021). For example, the interactions of some polar molecules with endohedral metallo C_{80} fullerene was investigated by Jalbout *et al.* (Jalbout, 2009) who considered interaction energy of H_2O, CH_3OH, HF and NH_3 molecules with endohedral metallo fullerene. Recently, Bucher *et al.* (Bucher, 2012) have reported the behavior of water trapped C_{60} fullerene. They indicated that the interaction of water with the carbon cage is weak. Also, Neyts *et al.* (Baei et al., 2011) have studied the interaction of dopant atom trapped inside and bound outside to the carbon cage (endo- and exohedral) or the metal atom via substituting one carbon atom. The adsorption energy of SCN^- on the exterior surfaces of C, BN, BP, AlN, and AlP nanostructures have been reported (Soltani et al., 2012; Soltani et al., 2012; Soltani et al., 2014; Kanani et al., 2014; Frisch et al., 2009). Herein this work, the adsorption behavior and electronic structures of interacting SCN^- towards the exterior surfaces of pristine and doped C_{60} nanostructures were examined to provide further insights on designing novel gas sensor materials.

2. Computational details

The equilibrium geometry, natural bond orbital (NBO), and density of states (DOS) calculations were performed (Alireza, 2012) through Gaussian 09 suite of programs (Cao et al., 2021). B3LYP level (Soltani et al., 2017; Soltani et al., 2018; Baei et al., 2014; Kia et al., 2013) was used for geometry development through the 6-31G** basis set. B3LYP/6-31G** level of theory were illustrated as a dependable and usually utilized level to evaluate of carbon fullerenes (Baei et al., 2017; Baei et al., 2017; Hassani and Tavakol, 2014). Three additional nanostructures were examined by substituting one carbon atom in C_{60} with one Al, Ga or B atom to form doped C_{60} heterofullerenes. The adsorption energies (E_{ad}) of SCN^- on the nanostructures of C_{60}, $C_{59}Al$, $C_{59}Ga$, $C_{59}B$ were determined through the following equation:

$$E_{ad} = E_{nanostructure-SCN} - (E_{nanostructure} + E_{SCN^-}) \quad (1)$$

where $E_{nanostructure-SCN}$, $E_{nanostructure}$, E_{SCN} are the total energies of adsorption complexes, pristine nanostructures and free SCN^-. The adsorption energy has been performed for the basis set superposition error (BSSE) in the most stable states by the full counterpoise method. Natural charge analysis with complete NBO calculations was performed by the B3LYP/6-31G** level of theory for relaxed structures (Wang et al., 2022). Quantum molecular descriptors like ionization potential (I), electron affinity (A), chemical potential (μ), global hardness (η), global softness (S) and electrophilicity index (ω) (Taibi, 2021) (Alireza, 2012) have been computed to predict the physical and chemical features of adsorption complexes, pristine nanostructures and isolated SCN^- (Cao et al., 2021; Soltani et al., 2022; Sun et al., 2022; Gallo et al., 1997). The I and A amounts have been studied as the negative of HOMO and LUMO energies, respectively, based on Koopmans' approximation (Serkan, 2020).

3. Result and discussion

3.1. Adsorption state of SCN^- on the carbon nanocages

Based on present computational analysis, the bond lengths of C_1-C_2 and C_1-C_3 in the pure C_{60} are about 1.395 and 1.453 Å with sp^2 hybridization (Fig. 1). The outputs are similar to the results which is reported by Gallo and co-worker (Chen et al., 2021). After adsorption of SCN through N-down on carbon atom of C_{60} (Fig. 1b), the bond lengths of C_1-C_2 and C_1-C_3 in this complex changed to 1.511 and 1.548 Å. These results

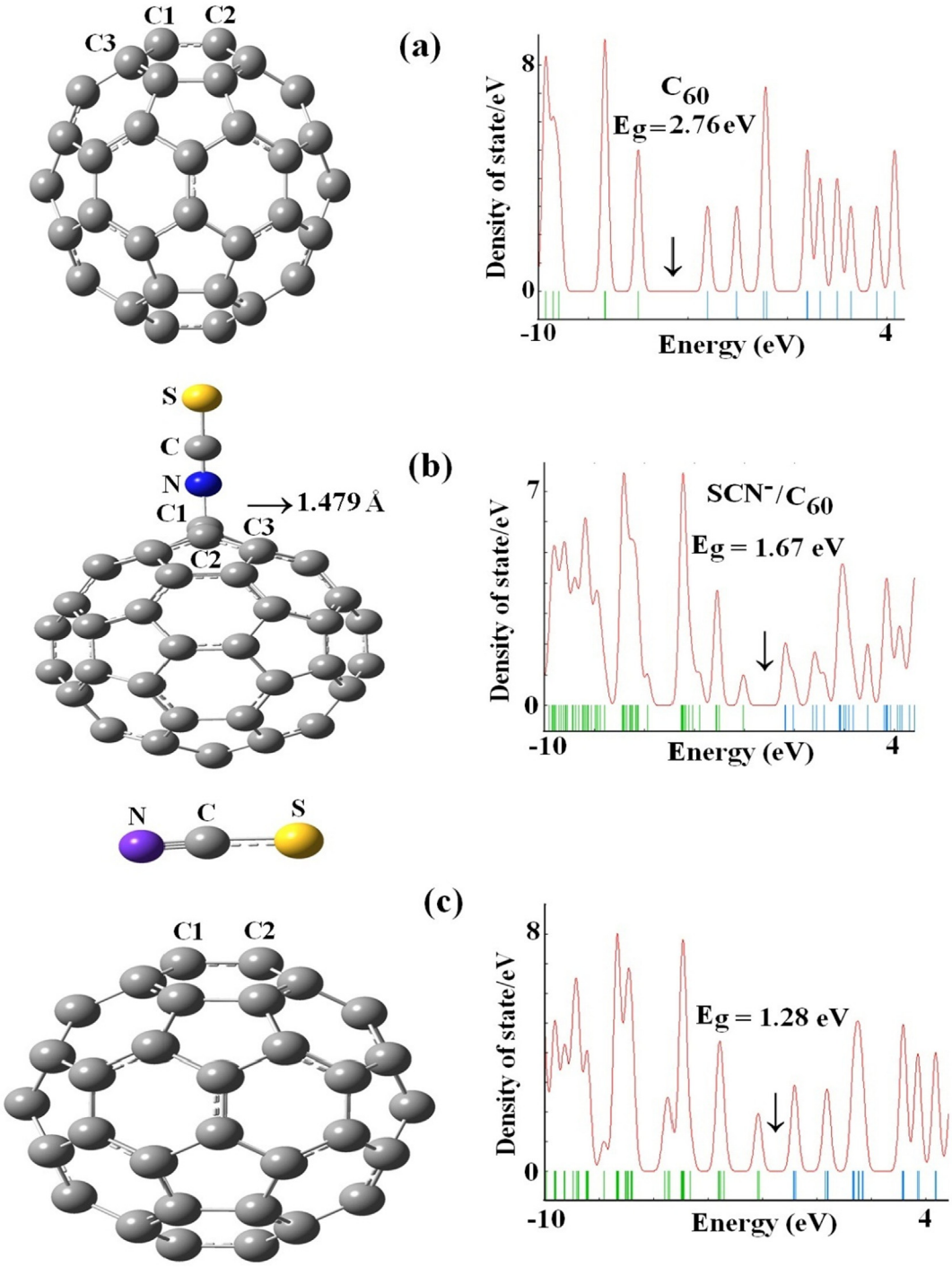

Fig. 1 The relaxed structures and density of states for the pure C_{60} and SCN^- interacting with C_{60} systems in different positions.

imply that the adsorption of SCN^- on the wall of the pristine C_{60} has noticeable influence on bond lengths of carbon atoms (Peyghan et al., 2013). The most stable configuration for the SCN^- adsorption (*N*-down) on the pristine C_{60} has adsorption energy of -48.06 kJ mol^{-1} and the interaction distance is 1.479 Å. Similarly, the most stable configuration for the SCN^- adsorption (parallel position) over the pristine C_{60} has adsorption energy of -52.41 kJ mol^{-1} and the interaction distance is 2.53 Å. After the use of BSSE calculation, the values of E_{ads} for the SCN^- adsorption through *N*-down and parallel position on the pristine C_{60} have adsorption energies of -43.21 and -47.08 kJ mol^{-1}, suggesting the nature of this the interaction in the terms of E_{ad} has mainly electrostatic character. Upon the adsorption of SCN^- with C_{60} fullerene (Fig. 1c), the average distances of C_1-C_2 and C_1-C_3 change to sp^3 hybridization of lengths 1.51 and 1.54 Å while the bond lengths of C—N and C—S upon the adsorption of SCN^- on the wall of fullerene is 1.186 and 1.607 Å, respectively. For this system, the results of NBO analysis exhibits that there is large charge transfer (0.70 e) from SCN^- to the surface of C_{60} full-

erene. Moreover, the computed adsorption energy of SCN^- toward the wall of fullerene is obviously higher than those on the surfaces of CNT and BNNT (Soltani et al., 2012; Soltani et al., 2012). The previous report represents that the value of E_{ad} for the SCN^- on the perfect (6, 0) BNNT was −148 kJ mol^{-1} (Soltani et al., 2012) and it increased on the outer surfaces of the AlPNT (−318.163 kJ mol^{-1}), AlNNT (−262.145 kJ mol^{-1}), and BPNT (−255.845 kJ mol^{-1}) (Soltani et al., 2014). It is observed from the outputs that the adsorption behavior of SCN^- on the fullerene surface is weak electrostatic interaction. While the E_{ad}value for the SCN^- on BNNT, BPNT, AlPNT, and AlNNT surfaces are chemisorption and a covalent bound is expected to produce through interaction of each configuration with SCN^- (Soltani et al., 2014; Frisch et al., 2009). Our last investigation on the effect of doping atoms on chemical interaction encouraged us to scrutinizing it on fullerene (Figs. 2 and 3).

The computations of SCN^- corresponding to $C_{59}B$, $C_{59}Al$, and $C_{59}Ga$ fullerenes confirmed our expectation with adsorption amount of −258.28, −389.10, and −347.71 kJ mol^{-1} respectively, with the interaction distances of 1.52, 1.85, and 1.90 Å (Figs. 2 and 3). Outcomes verifying a chemisorption process as SCN^- close to $C_{59}B$, $C_{59}Al$, and $C_{59}Ga$ fullerenes. The adsorption and interaction distance of SCN^- through S-down attached to $C_{59}Al$ fullerene in order are −308.11 kJ mol^{-1} and 2.31 Å. In contrast, the increment in the interaction of

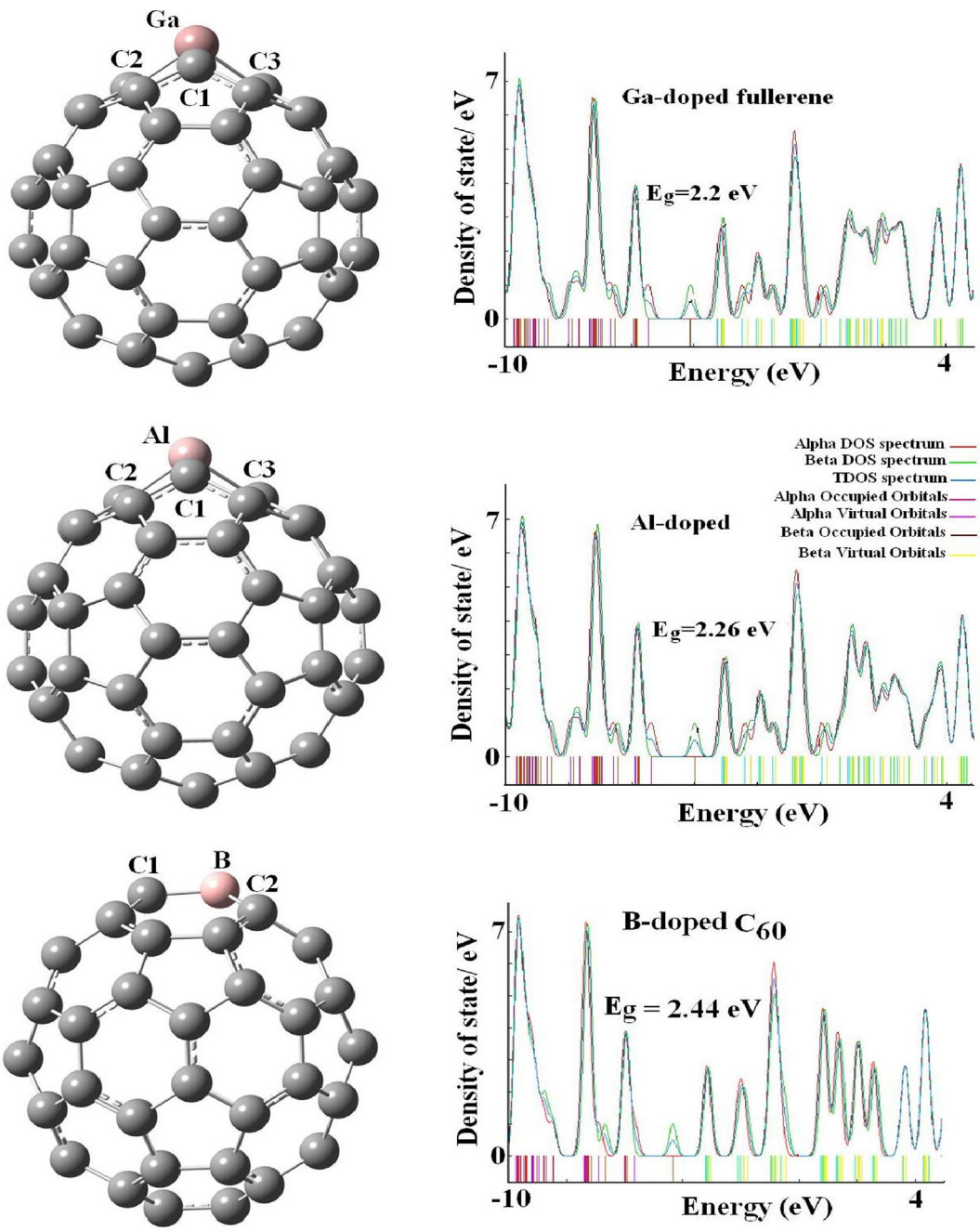

Fig. 2 The relaxed structures and density of states for the pure Ga-, Al-, and B-C_{59} systems.

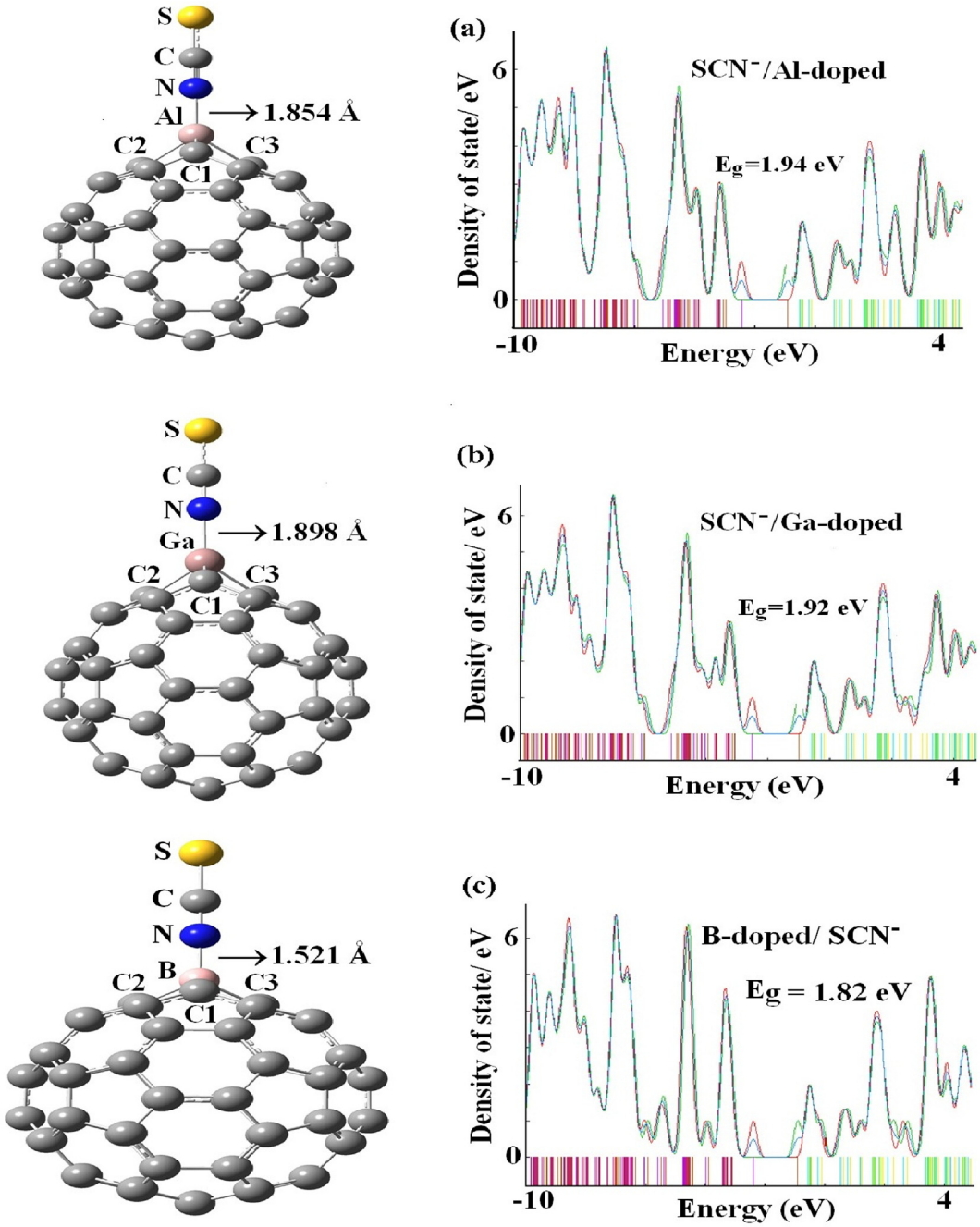

Fig. 3 The relaxed structures and density of states for the most stable state (*N*-down) of (a) $SCN^-/C_{59}Al$, (b) $SCN^-/C_{59}Ga$, and (c) $SCN^-/C_{59}B$ systems.

SCN^- with $C_{59}B$, $C_{59}Ga$, and $C_{59}Al$ fullerenes can be ascribed to the strong hybridization between dopant *p* orbitals of fullerene and the nitrogen *p* orbitals of anion. Moreover, the doping of Al can further enhance the adsorption of SCN^- onto the fullerene in comparison with the B- and Ga dopant atoms (Einert et al., 2021). These days, different significant approaches like functionalization, doping and size-dependent were applied in order to enhance or control the attributes of substances (Kurban et al., 2021; Muz et al., 2022; Muz et al., 2020; Olea Ullo et al., 2018; Soltani et al., 2016, 1105). To better understand the adsorption results, we performed the charge analysis which shows a strong charge transfer of approximately 0.50, 0.32, and 0.29 $|e|$ from the SCN^- to the $C_{59}B$, $C_{59}Ga$, and $C_{59}Al$ fullerenes. The analysis of NBO reveals that more ionic-bond-type process of electron transfer ameliorates the adsorption of SCN^- upon the $C_{59}B$, $C_{59}Ga$, and $C_{59}Al$ fullerenes. The strong chemical adsorption between the SCN^- and the $C_{59}B$, $C_{59}Ga$ and $C_{59}Al$ fullerenes leads to elongated bond lengths of B-C, Ga-C, and Al-C from 1.548, 1.887, and 1.884 Å to 1.616, 1.942, and 1.950 Å after the adsorption processes, respectively. The calculation thus exhibits that adsorbed N atom of SCN^- on $C_{59}B$, $C_{59}Ga$, and $C_{59}Al$ fullere-

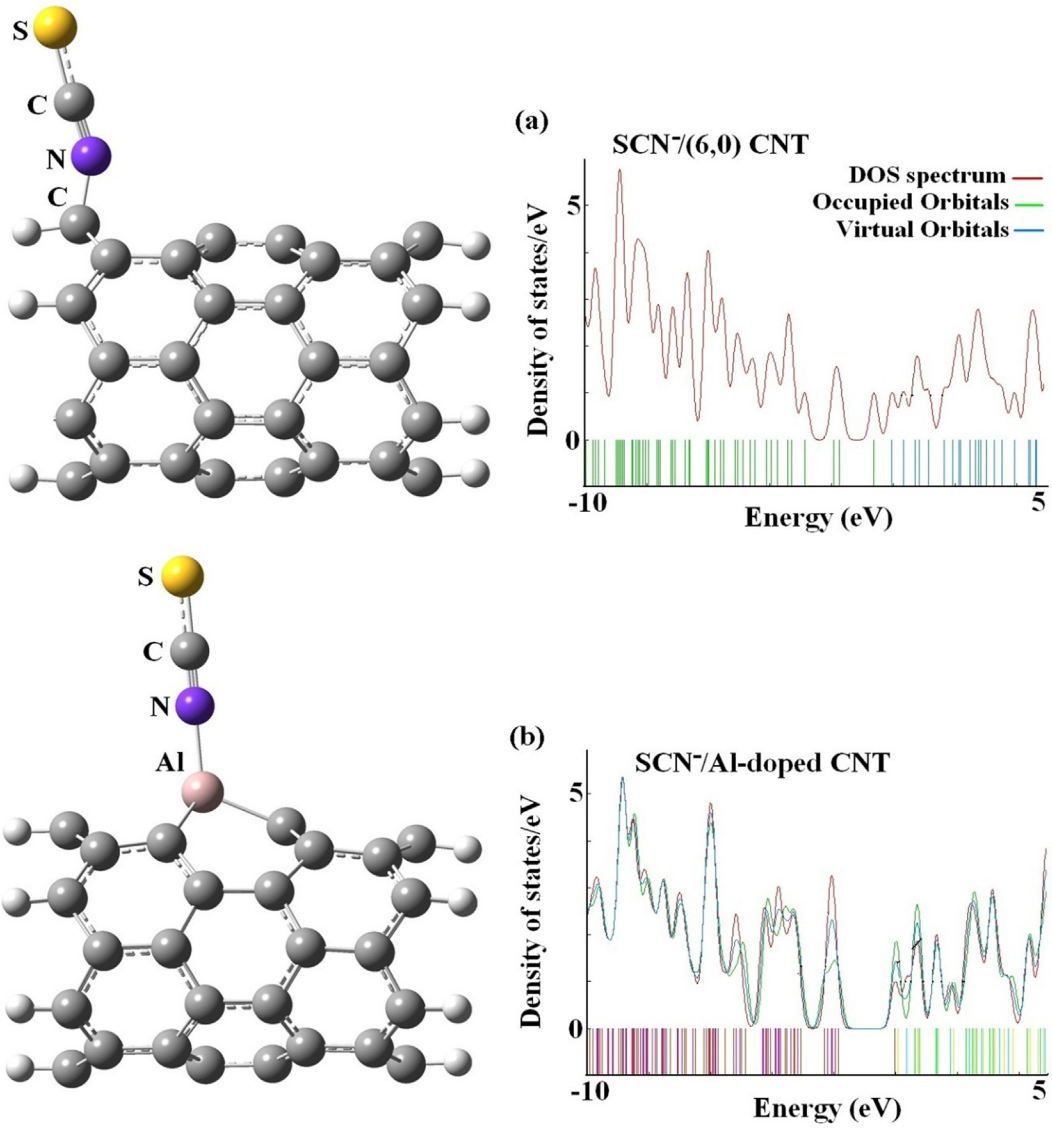

Fig. 4 The relaxed structures and density of states for the most stable state (*N*-down) of (a) SCN^-/(6,0) SWCNT and (b) SCN^-/Al-SWCNT systems.

nes had strong covalent bonds. The evaluation of our previous study (adsorption of SCN^- on the pure and Al-doped SWCNTs) exhibited that the single point energy (SPE) cannot purvey significant validity because of the lack of geometry relaxation of complexes provided (Soltani et al., 2012). According to our calculations (Fig. 4), the adsorption of SCN^- through *N*-down on the pure and Al-doped SWCNTs are −173.13 and −334.43 kJ mol^{-1}, suggesting that the SCN^- can be chemically bonded on the surface of Al-doped CNTs. Based on SPE calculations, the adsorption of SCN^- on the pure and Al-doped SWCNTs are found to be −26.08 and −286.38 kJ mol^{-1}, respectively (Soltani et al., 2012). On the SCN^- adsorption with SWCNT (Fig. 4a), the average distances of C_1-C_2 and C_1-C_3 shift to sp^3 hybridization of lengths 1.42 and 1.44 Å while the bond lengths of C—N and C—S upon the adsorption of SCN^- on the wall of nanotube in order is 1.185 and 1.604 Å (Ramezanitaghartapeh et al., 2022).

3.2. Electronic features

Considering the HOMO (high occupied molecular orbital) and the LUMO (low unoccupied molecular orbital), the most effective HOMO and LUMO (Rimadani, 2020) distribution plots for every form are proven in Fig. 5. The electro-positive and electro-negative densities, illustrated in order by the green and red colors, also are determined as almost equivalent in every shape.

Fig. 5 exhibits that the HOMO for SCN^-/C_{60} is slightly located upon the S—C—N orbital and is uniformly distributed upon the carbon atoms of C_{60} in energy level of −2.05 eV. The LUMO is more located on the carbon–carbon orbitals in the center of the C_{60} in energy level of −0.38 eV (Mohammad, 2014). In contrast, the HOMO of SCN^- is more resided on the carbon atoms in the center and near of the $C_{59}Al$, $C_{59}Ga$, and $C_{59}B$, and is slightly located on electronegative

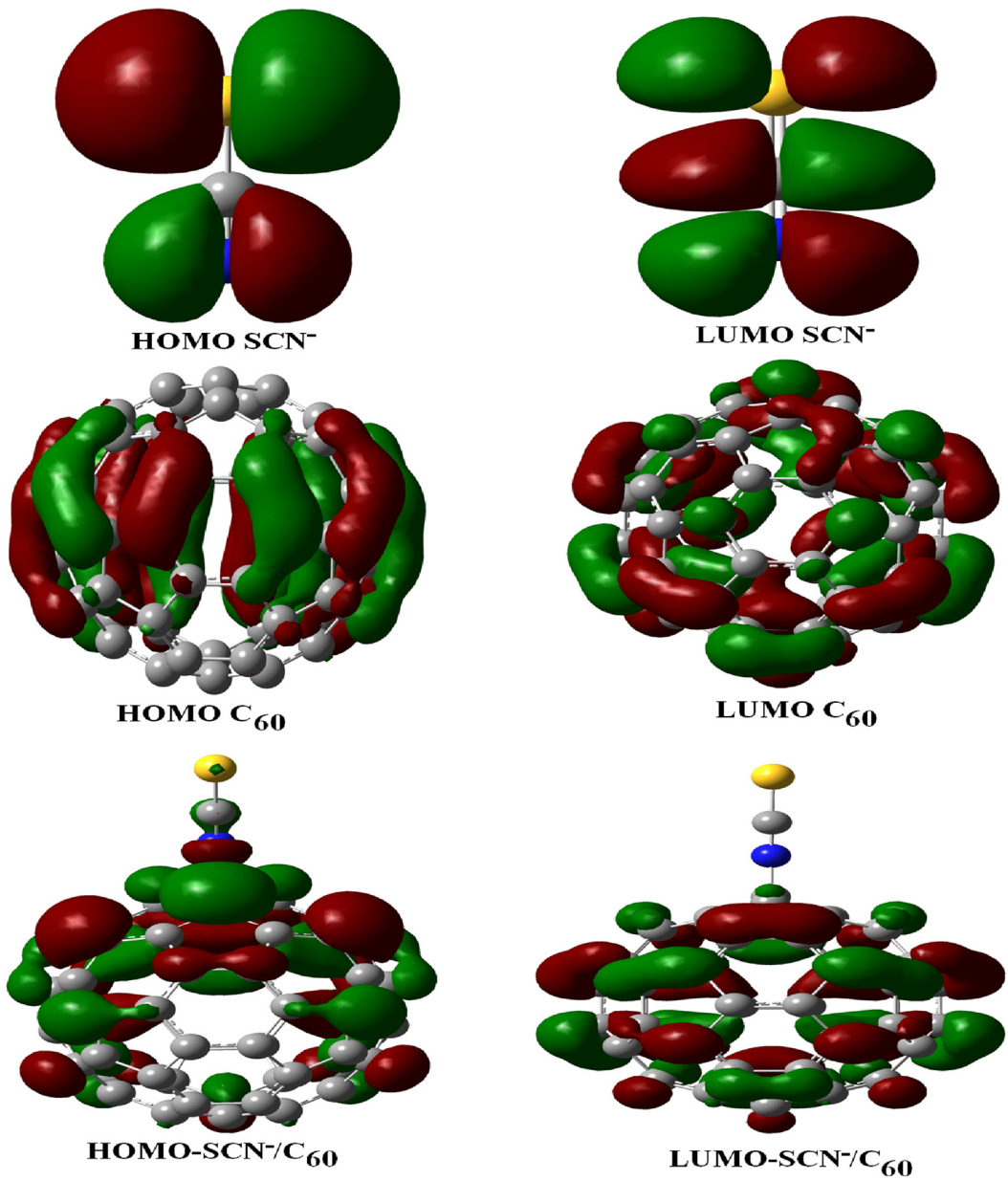

Fig. 5 Charge distribution of HOMO and LUMO orbitals upon the pure SCN^-, C_{60}, and, SCN^- adsorbed on C_{60}.

nitrogen atoms of SCN^- anion (Fig. 6) in energy levels of −2.45, −2.51, and −2.39 eV, while the LUMO orbitals for whole configurations are more dispensed upon the carbon–carbon bonds of fullerene cage in order in energy level of −0.51, −0.59, and −0.57 eV (Table 2). Fig. 7 presents the molecular electrostatic potential (MEP) map with an isodensity surface of 0.02 a.u. for pure C_{60} fullerene (B., 2022). Analysis of MEP represents that the blue color of the pristine C_{60} fullerene acts as electron-rich regions and the red color acts as the electron-poor regions (Avramopoulos et al., 2016).

As it is clear from the Table 1 and 2, there is a significant diminish in energy gaps from C_{60} to $C_{59}Al$, $C_{59}B$, and $C_{59}Ga$ fullerenes from 2.76 eV for C_{60} to 2.26, 2.20, and 2.44 eV for $C_{59}Al$, $C_{59}B$, and $C_{59}Ga$ fullerenes (Avramopoulos et al., 2016; Bahrami et al., 2014). The diminish is due to approaching of SCN^- to the exterior walls of $C_{59}Al$, $C_{59}B$, and $C_{59}Ga$ fullerenes with high reduced placing at $SCN^-/C_{59}B$ complex from 2.44 eV for basic stage to 1.82 eV for mixture plot, as gap energy for $C_{59}Al$ and $C_{59}Ga$ fullerenes in order are 1.94 and 1.92 eV. Also, the value of E_g is 2.67 eV for the mixture of SCN^- and C_{60}. Therefore, the reactivity of $C_{59}Al$, $C_{59}B$, and $C_{59}Ga$ fullerenes would be increased as SCN^- approaches to the aforementioned configurations. Therefore, unlike the $C_{59}Al$ and $C_{59}Ga$ fullerenes, the B-doping improves the sensitivity of the fullerene interacting with the SCN^- anion. The reduction of E_g improves the complexes electrical conductivity, which can then be converted to an electrical signal by $C_{59}B$ for SCN^-detection (Bahrami et al., 2014) (S.A., 2018).

C_{60} has icosahedral symmetry (I_h point group) and composed of sixty carbon atoms (Soltani et al., 2012). The symmetry of the $C_{59}Al$, $C_{59}B$, and $C_{59}Ga$ fullerenes is C_s, so their symmetry is not similar than for the C_{60} case, as SCN^- have

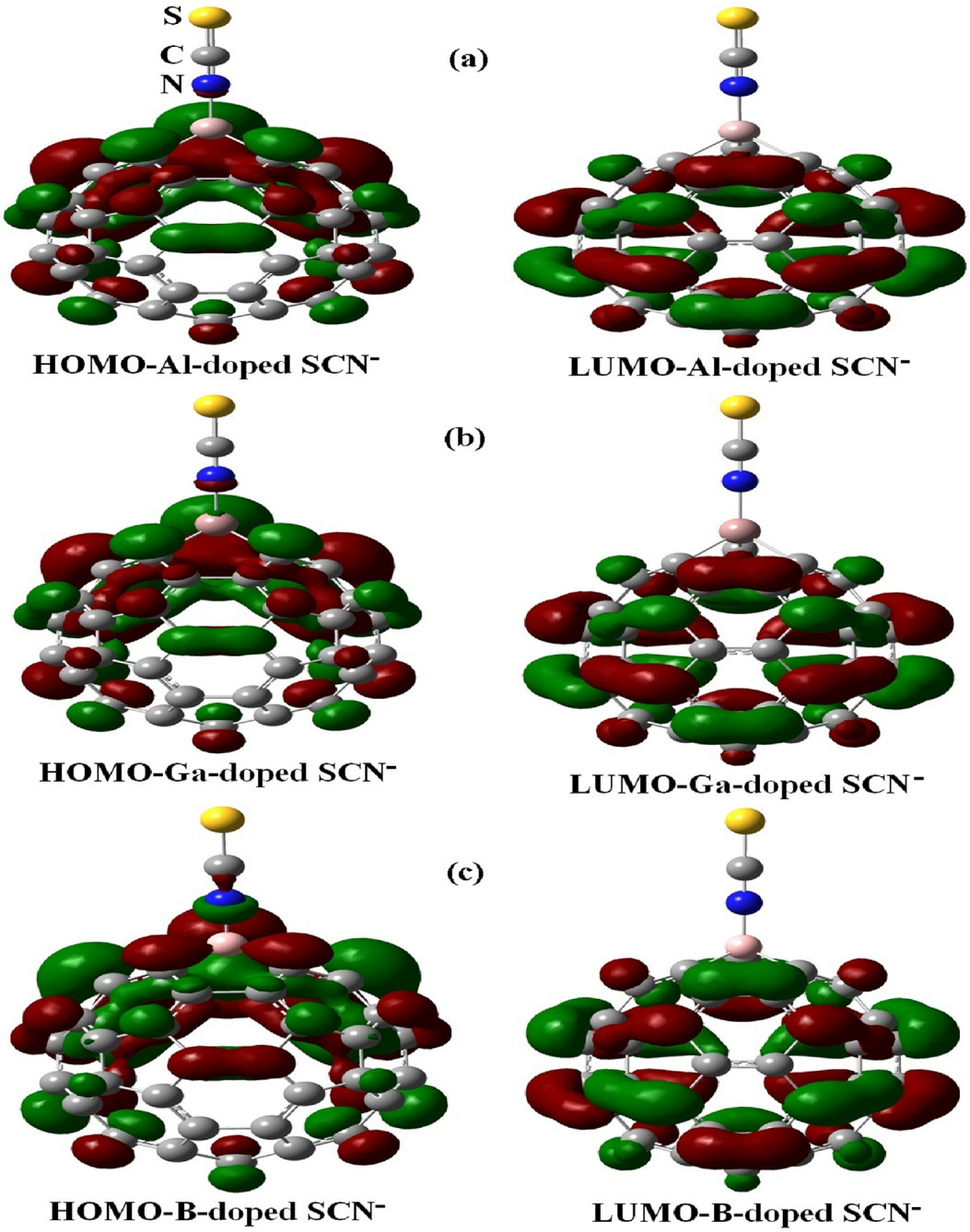

Fig. 6 Charge distribution of HOMO and LUMO orbitals upon the pure Ga-, Al-, and B-C_{59} loaded with one SCN^-.

Table 1 Calculated HOMO energies (E_{HOMO}/eV), LUMO energies (E_{LUMO}/eV), dipole moment (μ_D/Debye), and HOMO–LUMO energy gap ($E_{LUMO} - E_{HOMO}$/eV) for the pure and their complexes.

Property	SCN^-	C_{60}	SCN^-/C_{60}(*N*-down)	SCN^-/C_{60}(Parallel)
E_{HOMO}/eV	−5.38	−5.99	−2.05	−2.14
E_{LUMO}/eV	−3.12	−3.23	−0.38	−0.86
$[E_{LUMO} - E_{HOMO}]$/eV	2.26	2.76	1.67	1.28
$\mu_D/Debye$	2.64	0.00	8.27	34.40
E_F/eV	−4.25	−4.61	−1.21	−1.50
ΔE_g/eV	–	–	1.09	1.48

Table 2 Calculated HOMO energies (E_{HOMO}/eV), LUMO energies (E_{LUMO}/eV), dipole moment (μ_D/Debye), and HOMO–LUMO energy gap ($E_{LUMO} - E_{HOMO}$/eV) for the doped-C_{59} and their complexes.

Property	AlC59	SCN^-/C59Al	C59Ga	SCN^-/C59Ga	C59B	SCN^-/C59B
E_{HOMO}/eV	−5.38	−2.45	−5.44	−2.51	−5.66	−2.39
E_{LUMO}/eV	−3.12	−0.51	−3.24	−0.59	−3.22	−0.57
$[E_{LUMO} - E_{HOMO}]$/eV	2.26	1.94	2.20	1.92	2.44	1.82
$\mu_D/Debye$	2.64	18.35	1.61	30.01	0.573	19.75
E_F/eV	−4.25	−1.48	−4.34	−1.55	−4.44	−1.48
ΔE_g/eV	–	0.32	–	0.28	–	0.62

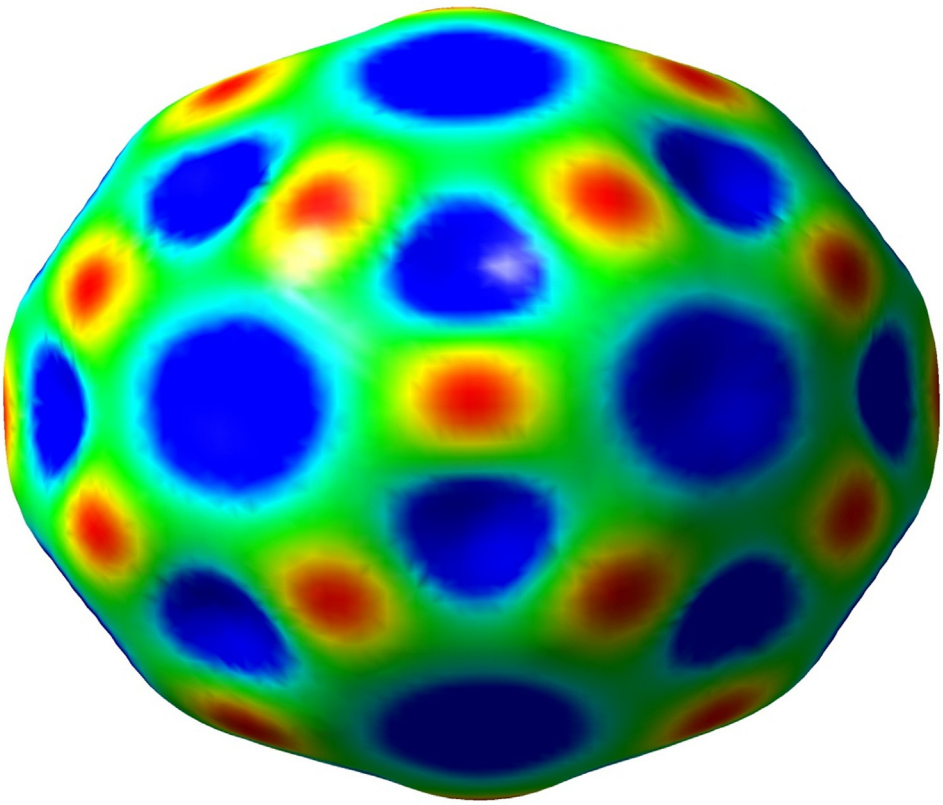

Fig. 7 MEP map of C_{60} fullerene.

C∞V symmetry. Besides, the point groups of SCN^- on C_{60}, $C_{59}Al$, $C_{59}B$, and $C_{59}Ga$ fullerenes are C1. NBO analysis demonstrates that the electronic configurations of $C_{59}Al$ and $C_{59}Ga$ models are [Ne] 3 $s^{0.33}3p^{0.39}$ and [Ar] 4 $s^{0.38}4p^{0.37}$, while $SCN^-/C_{59}Al$ and $SCN^-/C_{59}Ga$ models are of [Ne] 3 $s^{0.25}3p^{0.42}$ and [Ar] 4 $s^{0.63}4p^{0.99}$, respectively. Hence, the more reactivity has taken place the more charge transfer has occurred for SCN^- adsorbed on C_{60}, $C_{59}Al$, $C_{59}B$, and $C_{59}Ga$ fullerenes. A substantial characteristic that demonstrates the charge distribution when gases are adsorbed to the system is the dipole moment (μ_D) vector of species (Alireza, 2012). As a gas approaches or remotes from a fullerene, alteration of the size and direction of the μ_D is predictable. The results of the μ_D for whole configurations are scrutinized and speculated that total μ_D upraised drastically as SCN^- approaches to varied configuration of fullerene. Our calculations suggest that the dipole moment (μ_D) value for pure C_{60} and SCN^- are 0.00 and 2.64 Debye, respectively that with the adsorption of SCN^- in the positions of *N*-down and parallel both complexes in order increased to 8.27 and 34.40 Debye (Table 1). The μ_D values are found to be 1.61, 2.64, and 0.57 for $C_{59}Al$, $C_{59}Ga$, $C_{59}B$ fullerenes, respectively. While it significantly increased as a result of SCN^- closeness to the outer surface of considered configurations, with 18.35, 30.01, and 19.75 Debye for $C_{59}Al$, $C_{59}Ga$, $C_{59}B$ fullerenes (Table 2). To observe the adsorption behavior in these complexes, the DOS of SCN^-/C_{60} complex in comparison with other complexes including $SCN^-/C_{59}Al$, $SCN^-/C_{59}Ga$, and $SCN^-/C_{59}B$ was analyzed. As depicted in Figs. 1 and 3, the DOS of practical complexes are remarkably altered when the SCN^- adsorbed upon the surface of fullerene while it is more noticeable in pure model (parallel position). These data illustrate that DOS close the Fermi

Table 3 Calculated quantum molecular descriptors for the fullerene and their complexes.

Property	SCN^-	C_{60}	SCN^-/C_{60}	$C_{59}Al$	$SCN^-/C_{59}Al$	$C_{59}Ga$	$SCN^-/C_{59}Ga$
I/eV	0.41	5.99	2.05	5.38	2.45	5.44	2.51
A/eV	−7.41	3.23	0.38	3.12	0.51	3.24	0.59
η/eV	3.91	1.38	0.83	1.13	0.97	1.10	0.96
μ/eV	−3.50	−4.61	−1.21	−4.25	−1.48	−4.34	−1.55
S/eV^{-1}	0.13	0.36	0.60	0.44	0.51	0.45	0.52
ω/eV	1.57	7.69	0.89	7.99	1.13	8.56	1.25
ΔN_{max}/a.u.	1.65	−3.34	−1.46	3.76	−1.52	3.86	−1.61

level (EF) are influenced by the SCN^- and C_{60}, $C_{59}Al$, $C_{59}Ga$, and $C_{59}B$. Moreover, the great charge transfer is probable as extracted from EF outcomes revealing as basic amount of −4.61 eV for the pure C_{60} to −1.21 eV and −1.50 eV for SCN^- through *N*-down and parallel positions on the surface of C_{60} fullerene, respectively. The values of EF for the pure $C_{59}Al$, $C_{59}Ga$, and $C_{59}B$ are changed from −4.25, −4.34, and −4.44 eV to −1.48, −1.55, and −1.48 eV for SCN^- interacting with $C_{59}Al$, $C_{59}Ga$, and $C_{59}B$ systems, respectively. Our findings introduce fullerene and its doped models as high sensitivity materials to SCN^- that resemble a gas sensor.

3.3. Scrutinizing of quantum molecular descriptor for SCN^-

Results of Quantum Molecular Descriptor (QMD) represents a decrement on energy gap (E_g: [E_{LUMO} − E_{HOMO}]) that results in ionization potential increase from 2.05 eV for SCN^- approaching to pure C_{60} to 2.45 and 2.51 eV for $C_{59}Al$ and $C_{59}Ga$ respectively, and consequently raise in global hardness (η) from 0.83 eV for SCN^- on the pristine complex to 0.97 and 0.96 eV for $C_{59}Al$ and $C_{59}Ga$ when SCN^- is added to them. Similar plot is predictable for electron affinity (A) with 0.51 and 0.59 eV for SCN^- on the surfaces of the $C_{59}Al$ and $C_{59}Ga$ fullerenes from basic amount of 0.38 eV for SCN^- approaching to perfect $C_{60.}$ Chemical potential (μ) increased from 1.21 eV for pure matrix of SCN/C_{60} to 1.48 and 1.55 eV for $SCN/C_{59}Al$ and $SCN/C_{59}Ga$ complexes. An increase in electrophilicity index (ω) for SCN^-/Ga-doped C_{59} complex is noticeable than that of $SCN/C_{59}Al$ complex with certain amount of 1.25 eV. Considering softness (S), it has decreased from 0.60 eV at SCN^-/C_{60} complex to 0.51 eV and 0.52 eV for $SCN/C_{59}Al$ and $SCN/C_{59}Ga$ complexes, respectively (see Table 3).

4. Conclusion

SCN^- adsorption capacity on outer surface of perfect C_{60} in comparison with $C_{59}B$, $C_{59}Al$, and $C_{59}Ga$ fullerenes have been investigated through density functional theory calculations. Then interaction of the SCN^- with $C_{59}Al$ is covalent in nature with the strong adsorption energy about −389.10 kJ mol^{-1}. These results indicate that the chemisorption of SCN^- on surface of $C_{59}Al$ with a strong charge transfer about 0.29 e. Our computation study shows that the adsorption property of SCN^- on the $C_{59}Al$ surfaces is most notable as compared to $C_{59}Ga$ and $C_{59}B$ for SCN^- storages. Moreover, the eligible $C_{59}Al$ nano-cage has significant energetic endurances and slightly larger energy gaps than the dopant Ga and B atoms. Therefore, the presence of $C_{59}B$, $C_{59}Al$, and $C_{59}Ga$ fullerenes can lower the electrophilicity, ionization potential, energy gaps and then upraise the softness or global hardness with the adsorption properties of SCN^-.

Declaration of Competing Interest

The authors declare that they have no known competing financial interests or personal relationships that could have appeared to influence the work reported in this paper.

Acknowledgements

–Rami M. Alzhrani would like to acknowledge Taif University Researchers Supporting Project Number (TURSP-2020/209), Taif University, Taif, Saudi Arabia.

–The authors would like to thank the Deanship of Scientific Research at Umm Al-Qura University for supporting this work by Grant Code :(22UQU4290565DSR98).

References

Alireza, Soltani, 2012. Ab initio investigation of Al- and Ga-doped single-walled boron nitride nanotubes as ammonia sensor. Applied surface science. https://doi.org/10.1016/j.apsusc.2012.09.122.

Alireza, Soltani, 2012. Ab initio investigation of Al- and Ga-doped single-walled boron nitride nanotubes as ammonia sensor. applied surface science. https://doi.org/10.1016/j.apsusc.2012.09.122.

Avramopoulos, A., Otero, N., Karamanis, P., Pouchan, C., Papadopoulos, M.G., 2016. A Computational Study of the Interaction and Polarization Effects of Complexes Involving Molecular Graphene and C_{60} or a Nucleobases. J. Phys. Chem. A 120 (2), 284–298.

Baei, M.T., Soltani, A., Torabi, P., Varasteh Moradi, A., 2011. Adsorption properties of SCN- on (6,0), (7,0), (8,0), and Al-doped (6,0) zigzag single-walled carbon nanotubes: A density functional study. Monatshefte 142, 979–984.

Baei, M.T., Soltani, A., Hashemian, S., Mohammadian, H., 2014. $Al_{12}N_{12}$ nanocage as a potential sensor for phosgene detection. J. Chem. 92, 605.

Baei, M.T., Soltani, A., Rajabzadeh, H., Tazikeh-Lemeski, E., 2017. Structural and Electronic Properties of XY-Doped (AlN, AlP, GaN, GaP) C_{58} Fullerenes: a DFT Study. Russ. J. Inorg. Chem. 62, 1067–1076.

B., Gassoumi, 2022. Spectroscopic characterization, host-guest charge transfer, Hirshfeld surfaces, AIM-RDG and ELF study of adsorption and chemical sensing of heavy metals with new derivative of Calix [4]quinone: A DFT-D3 computation. Materials Chemistry and physics.

Baei, M.T., Ramezani Taghartapeh, M., Soltani, A., Hosseni Amirabadi, K., Gholami, N., 2017. Interaction of Pure and Metal Atom Substituted Carbon Nanocages with CNCl: a DFT Study, Russian. J. Phys. Chem. B 11, 354–360.

Bahrami, A., Yourdkhani, S., Esrafilib, M.D., Hadipour, N.L., 2014. A DFT study on doping assisted changing of B_{80} electronic structure: Promising candidates for NH_3 sensor. Sens. Actuators, B 191, 457–463.

Bakry, R., Vallant, R.M., Najam-ul-Haq, M., Rainer, M., Szabo, Z., Huck, C.W., et al, 2007. Medicinal applications of fullerenes. Int. J. Nanomed. 2, 639–649.

Bezi Javan, M., Tajabor, N., Behdani, M., Rezaee Rokn-Abadi, M., 2010. Influence of 3d transitionmetals (Fe, Co) on the structural, electrical and magnetic properties of C_{60} nano-cage. Phys. B 405, 4937–4942.

Bucher, D., 2012. Orientational relaxation of water trapped inside C_{60} fullerenes. Chem. Phys. Lett. 534, 38–42.

Cao, Y., Khan, A., Mirzaei, H., Khandoozi, S.R., Javan, M., Ng Kay Lup, A., Norouzi, A., Tazikeh Lemeski, E., Pishnamazi, M., Soltani, A., Albadarin, A.B., 2021. Investigations of adsorption behavior and anti-cancer activity of curcumin on pure and platinum-functionalized B12N12 nanocages. J. Mol. Liquids 334.

Cao, Y., Khan, A., Balakheyli, H., Lup, A.N.K., Ramezani Taghartapeh, M., Mirzaei, H., Reza Khandoozi, S., Soltani, A., Aghaei, M., Heidari, F., Sarkar, S.M., Albadarin, A.B., 2021. Penicillamine functionalized $B_{12}N_{12}$ and $B_{12}CaN_{12}$ nanocages act as potential inhibitors of proinflammatory cytokines: A combined DFT analysis, ADMET and molecular docking study. Arab. J. Chem. 14 (7), 103200.

Chen, D., Szczepanik, D.W., Zhu, J., Muñoz-Castro, A., Solà, M., 2021. Aromaticity Survival in Hydrofullerenes: The Case of $C_{66}H_4$ with Its π-Aromatic Circuits. Chem. Eur. J. 27 (2), 802–808.

Einert, M., Hartmann, P., Smarsly, B., Brezesinski, T., 2021. Quasi-homogenous photocatalysis of quantum-sized Fe-doped TiO_2 in optically transparent aqueous dispersions. Sci. Rep. 11, 17687.

Frisch, M.J., Trucks, G.W., Schlegel, H.B., Scuseria, G.E., Robb, M. A., Cheeseman, J.R., Montgomery Jr., J.A., Vreven, T., Kudin, K. N., Burant, J.C., Millam, J.M., Iyengar, S.S., Tomasi, J., Barone, V., Mennucci, B., Cossi, M., Scalmani, G., Rega, N., Petersson, G. A., Nakatsuji, H., Hada, M., Ehara, M., Toyota, K., Fukuda, R., Hasegawa, J., Ishida, M., Nakajima, T., Honda, Y., Kitao, O., Nakai, H., Klene, M., Li, X., Knox, J.E., Hratchian, H.P., Cross, J. B., Bakken, V., Adamo, C., Jaramillo, J., Gomperts, R., Stratmann, R.E., Yazyev, O., Austin, A.J., Cammi, R., Pomelli, C., Ochterski, J.W., Ayala, P.Y., Morokuma, K., Voth, G.A., Salvador, P., Dannenberg, J.J., Zakrzewski, V.G., Dapprich, S., Daniels, A.D., Strain, M.C., Farkas, O., Malick, D.K., Rabuck, A. D., Raghavachari, K., Foresman, J.B., Ortiz, J.V., Cui, Q., Baboul, A.G., Clifford, S., Cioslowski, J., Stefanov, B.B., Liu, G., Liashenko, A., Piskorz, P., Komaromi, I., Martin, R.L., Fox, D. J., Keith, T., AlLaham, M.A., Peng, C.Y., Nanayakkara, A., Challacombe, M., Gill, P.M.W., Johnson, B., Chen, W., Wong, M. W., Gonzalez, C., Pople, J.A., 2009. Gaussian 09, Revision A01. Gaussian, Inc., Wallingford, CT.

Funasaka, H., Sakurai, K., Oda, Y., Yamamoto, K., Takahashi, T., 1995. Magnetic properties of $Gd@C_{82}$ metallofullerene. Chem. Phys. Lett. 232, 273–277.

Gallo, E., Solari, E., Re, N., Floriani, C., Chiesivilla, A., Rizzoli, C., 1997. Carbon-carbon bonds functioning as electron shuttles: The generation of electron-rich manganese(II) Schiff base complexes and their redox chemistry. J. Am. Chem. Soc. 119, 5144–5154.

Hassani, F., Tavakol, H., 2014. A DFT, AIM and NBO study of adsorption and chemical sensing of iodine by S-doped fullerenes. Sens. Actuators, B 196, 624–630.

Hernández, A.B., Hernandez, W.I., Severiano, F., Hernandez, E.G., Chigo Anota, E., Salazar Villanueva, M., 2021. Physical-chemical properties of $(Znm)@C_{60}$ and $(Znm)@C_{70}$ endohedral metallofullerenes (m = 1–5): A DFT approach. Surf. Interfaces 23, 101012.

Iijima, S., 1991. Helical microtubules of graphitic carbon. Nature 354, 56–58.

Jalbout, A.F., 2009. Endohedral metallo [80] fullerene interactions with small polar molecules. Comput. Mater. Sci. 44, 1065–1070.

Kanani, Y., Baei, M.T., Moradi, A.V., Soltani, A., 2014. Adsorption mechanism of single OCN^- and SCN^- upon single-walled BP nanotubes. Phys. E 59, 66–74.

Kia, M., Golzar, M., Mahjoub, K., Soltani, A., 2013. A first-principles study of functionalized clusters and carbon nanotubes or fullerenes with 5-Aminolevulinic acid as vehicles for drug delivery. Superlatt. Microstruct. 62, 251–259.

Krainara, N., Illas, F., Limtrakul, J., 2012. Interaction of adenine Cu (II) complexes with BN-doped fullerene differentiates electronically equivalent tautomers. Chem. Phys. Lett. 537, 88–93.

Kroto, W., Heath, J.R., O'Brien, S.C., Curl, R.F., Smalley, R.E., 1985. C_{60}: buckminsterfullerene. Nature 318, 162–163.

Kurban, H., Alaei, S., Kurban, M., 2021. Effect of Mg content on electronic structure, optical and structural properties of amorphous ZnO nanoparticles: A DFTB study. J. Non-Crystall. Solids 560. 120726(1–6).

Larssona, J.A., Greer, J.C., 2002. Phosphorous trapped within buckminsterfullerene. J. Chem. Phys. 116, 7849–7854.

Liu, F.-L., 2009. Heterofullerene molecules $C_{58}X$ (X = S, Se, Te): A DFT study. Chem. Phys. Lett. 471, 116–121.

Liu, F.-L., Li, J., Zhang, H., 2008. DFT study of a heterofullerene molecule containing fifty-eight carbon atoms and one sulphur atom. Chem. Phys. 353, 19–24.

Mauser, H., van Eikema Hommes, N.J.R., Clark, T., Hirsch, A., Pektzak, B., Weidinger, A., Dunsch, L., 1997. Stabilization of atomic nitrogen inside C_{60}. Angew. Chem. Int. Ed. Engl. 36, 2835–2838.

Mohammad, T. Baei, 2014. Computational study of OCN^-chemisorption over AlN nanostructures. Superlattices and Microstructures.

Murata, M., Murata, Y., Komatsu, K., 2006. Synthesis and properties of endohedral C_{60} encapsulating molecular hydrogen. J. Am. Chem. Soc. 128, 8024–8033.

Muz, İ., Göktaş, F., Kurban, M., 2020. 3d-transition metals (Cu, Fe, Mn, Ni, V and Zn)-doped pentacene π-conjugated organic molecule for photovoltaic applications: DFT and TD-DFT calculations. Theor. Chem. Acc. 139, 23.

Muz, İ., Göktaş, F., Kurban, M., 2022. A density functional theory study on favipiravir drug interaction with BN-doped C_{60} heterofullerene. Physica E 135, 114950.

Neyts, E., Maeyens, A., Pourtois, G., Bogaerts, A., 2011. A density-functional theory simulation of the formation of Ni-doped fullerenes by ion implantation. Carbon 49, 1013–1017.

Olea Ullo, C., Ponce-Vargas, M., Muñoz-Castro, A., 2018. Formation of Coinage-Metal···Fullerene Adducts. Evaluation of the Interaction Nature between Triangular Coinage Metal Complexes (M_3 = Cu, Ag, and Au) and C_{60} through Relativistic Density Functional Theory Calculations. J. Phys. Chem. C 122 (43), 25110–25117.

Peyghan, A.A., Baei, M.T., Hashemian, S., Torabi, P., 2013. Adsorption of CO molecule on AlN nanotubes by parallel electric field. J. Mol. Model. 19 (2), 859–870.

Ramezanitaghartapeh, M., Achazi, A.J., Soltani, A., Miŕoc, P., Kaghazchi, P., Mahon, P.J., Hollenkamp, A.F., Musameh, M., 2022. Sustainable cyanide-C_{60} fullerene cathode to suppress the lithium polysulfides in a lithium-sulfur battery. Sustain. Mater. Technol. 32, e00403.

Ren, X.-Y., Jiang, C.-Y., Wang, J., Liu, Z.-Y., 2008. Endohedral complex of fullerene C_{60} with tetrahedrane, $C_4H_4@C_{60}$. J. Mol. Graph. Model. 27, 558–562.

Ren, Y.X., Ng, T.Y., Liew, K.M., 2006. State of hydrogen molecules confined in C_{60} fullerene and carbon nanocapsule structures. Carbon 44, 397–406.

Rimadani, Pratiwi, 2020. Reactivity and Stability of Metalloporphyrin Complex Formation: DFT and Experimental Study. MDPI.

Rondeau-Gagne, S., Curutchet, C., Grenier, F., Scholes, G.D., Morin, J.-F., 2010. Synthesis, characterization and DFT calculations of new ethynyl-bridged C_{60} derivatives. Tetrahedron 66, 4230–4242.

S.A., Javarsineh, 2018. A Computational Study on the Purinethol Drug Adsorption on the AlN Nanocone and Nanocluster. Scientific reports.

Sabirov, D.S., Khursan, S.L., Bulgakov, R.G., 2008. Ozone addition to C_{60} and C_{70} fullerenes: A DFT study. J. Mol. Graph. Model. 27, 124–130.

Serkan, Caliskan, 2020. Structural, Electronic and Adsorption Characteristics of Transition Metal doped TM@C_{70} Endohedral Fullerenes. Communications biology.

Shi, J., Chen, Z., Wang, L., Wang, B., Xu, L., Hou, L., Zhang, Z., 2016. A tumor-specific cleavable nanosystem of PEG-modified C_{60}@Au hybrid aggregates for radio frequency-controlled release, hyperthermia, photodynamic therapy and X-ray imaging. Acta Biomater. 29, 282–297.

Shinohara, H., 2000. Endohedral metallofullerenes. Rep. Prog. Phys. 63, 843–892.

Soltani, A., Taghartapeh, M.R., Mighani, H., Pahlevani, A.A., Mashkoor, R., 2012. A first-principles study of the SCN^- chemisorption on the surface of AlN, AlP, and BP nanotubes. Appl. Surf. Sci. 259, 637–642.

Soltani, A., Ahmadian, N., Kanani, Y., Dehnokhalaji, A., Mighani, H., 2012. Ab initio investigation of the SCN^- chemisorption of single-walled boron nitride nanotubes. Appl. Surf. Sci. 258, 9536–9543.

Soltani, A., Baei, M.T., Tazikeh Lemeski, E., Allah, A., 2014. Pahlevani: The study of SCN^- adsorption on $B_{12}N_{12}$ and $B_{16}N_{16}$ nano-cages. Superlatt. Microstruct. 75, 716–724.

Soltani, A., Varasteh Moradi, A., Tazikeh Lemeski, E., 2016. The interaction of 2,6-dichlorobenzylidene-2,4-dichloroaniline (2,6-DBDA) and 2,4-dichlorobenzylidene-2,4-dichloroaniline (2,4-DBDA) with single-walled carbon nanotube: A DFT study. J. Mol. Struct. 1105, 128–134.

Soltani, A., Bezi Javan, M., Hoseininezhad-Namin, M.S., Tajabor, N., Tazikeh Lemeski, E., Pourarian, F., 2017. Interaction of hydrogen with Pd- and co-decorated C_{24} fullerenes: Density functional theory study. Synth. Met. 234, 1–8.

Soltani, A., Ramezani Taghartapeh, M., Erfani-Moghadam, V., Bezi Javane, M., Heidari, F., Aghaei, M., Mahon, P.J., 2018. Serine adsorption through different functionalities on the $B_{12}N_{12}$ and Pt-$B_{12}N_{12}$ nanocages. Mater. Sci. Eng., C 92, 216–227.

Soltani, A., Khan, A., Mirzaei, H., Onaq, M., Javan, M., Tavassoli, S., Mahmoodi, N.O., Arian Nia, A., Yahyazadeh, A., Salehi, A., Khandoozi, S.R., Masjedi, R.K., Rahman, M. L., Sarjadi, M.S., Sarkar, S.M., Su, C.-H., 2022. Improvement of anti-inflammatory and anticancer activities of poly(lactic-co-glycolic acid)-sulfasalazine microparticle via density functional theory, molecular docking and ADMET analysis. Arab. J. Chem. 15, 103464.

Sun, N., Ansari, M.J., Ng Kay Lup, A., Javan, M., Soltani, A., Khandoozi, S.R., Arian Nia, A., Tavassoli, S., Lutfor Rahman, M., Sani Sarjadi, M., Sarkar, S.M., Su, C.-H., Chinh Nguyen, H., 2022. Improved anti-inflammatory and anticancer properties of celecoxib loaded zinc oxide and magnesium oxide nanoclusters: A molecular docking and density functional theory simulation. Arab. J. Chem. 15.

Taibi, Ben Hadda, 2021. How to face COVID-19: proposed treatments based on remdesivir and hydroxychloroquine in the presence of zinc sulfate. Docking/DFT/POM structural analysis. Joiurnal of Biomolecular Structure and dynamics. https://doi.org/10.1080/07391102.2021.1930161.

Wang, Q., Zhang, P., Ansari, M.J., Aldawsari, M.F., Alalaiwe, A.S., Kaur, J., Kumar, R., Ng Kay Lup, A., Enayati, A., Mirzaei, H., Soltani, A., Su, C.-H., Chinh Nguyen, H., 2022. Electrostatic interaction assisted Ca-decorated C20 fullerene loaded to anti-inflammatory drugs to manage cardiovascular disease risk in rheumatoid arthritis patients. J. Mole. Liquids 350.

Wilson, L.J., 1999. Medical applications of fullerenes and metallofullerenes. Electrochem. Soc. Interface 8, 24–28.